

Semi-ballistic thermal conduction in polycrystalline SiGe nanowires

Noboru Okamoto¹, Ryoto Yanagisawa¹, Roman Anufriev¹, Md. Mahfuz Alam², Kentarou Sawano², Masashi Kurosawa^{3,4}, and Masahiro Nomura^{1,5*}

¹ Institute of Industrial Science, the University of Tokyo, Tokyo, 153–8505, Japan

² Advanced Research Laboratories, Tokyo City University, Tokyo, 158-0082, Japan
Nagoya, 464-8603, Japan

³ Graduate School of Engineering, Nagoya University, Nagoya 464–8603, Japan

⁴ Institute for Advanced Research, Nagoya University, Nagoya 464–8601, Japan

⁵ CREST, Japan Science and Technology Agency, Saitama, 332–0012, Japan

Ballistic heat conduction remains a controversial nanoscale phenomenon because of its occurrence and strength depends on the material, alloy composition, and temperature. Here, we discuss the impact of ballistic thermal conduction and compare the results with theoretical predictions. We experimentally investigate ballistic thermal transport in SiGe polycrystalline nanowires by measuring length dependence of thermal conductivity for different alloy compositions and temperatures. At room temperature, our experiments show that ballistic effects are negligible in nanowires made of pure polycrystalline Si but become stronger as Ge composition increases. As we decreased the temperature, we observed that ballistic contribution becomes even stronger.

Nanoscale thermal conduction in semiconductors can exhibit a curious deviation from a classical heat diffusion when phonons carrying heat experience no diffuse scattering events^{1–3}. In the absence of scattering, the thermal energy carried by the phonons travel without dissipation in straight lines for hundreds of nanometers until the next scattering event^{4,5}. This phenomenon is called ballistic heat conduction. In the fully ballistic limit, the thermal resistance (R) of the structure becomes independent on its length (L), thus the thermal conductivity ($\kappa \sim L / R$) loses its meaning of the intrinsic material property and becomes simply proportional to the length ($\kappa \sim L$). However, in a more general case, only a part of phonons carry heat without resistance and carry it over only a part of the structure. In this

*e-mail: nomura@iis.u-tokyo.ac.jp

This is the author's peer reviewed, accepted manuscript. However, the online version of record will be different from this version once it has been copyedited and typeset.

PLEASE CITE THIS ARTICLE AS DOI: 10.1063/1.5130659

semi-ballistic heat conduction regime, the thermal conductivity is proportional to L^a , where a is the coefficient that takes values between zero and one⁶.

The phenomenon of length-dependent thermal conductivity appeared in the experiments on various nanostructures and materials⁷⁻¹⁴. Particularly, some works¹⁰ suggested that the alloyed materials, such as SiGe nanowires (NWs), exhibit stronger ballistic conduction with the perfect length dependence $\kappa \sim L^1$ due to alloy scattering of high-frequency phonons. However, recent simulations⁶ of SiGe NWs showed much weaker length dependence with $\kappa \sim L^{0.33}$ despite the alloy scattering. Moreover, experiments on Si NWs typically show weak ballistic effects at room temperature but stronger effects at low temperatures of several kelvins^{9,15,16}. Thus, the picture of heat conduction in alloyed NWs and its temperature dependence remains incomplete.

In this work, we investigate ballistic thermal conduction in SiGe NWs with different alloy compositions and at different temperatures. We demonstrate that the thermal conductivity of short NWs becomes length-dependent. Analyzing this length dependence, we observe how the ballistic effects strengthen at lower temperatures and for higher Ge concentration.

To measure the thermal conductivity of SiGe NWs, we use micro time-domain thermoreflectance (μ TDTR) method. In the optical pump-probe technique, a suspended island with an aluminum pad is periodically excited by short pulses of the pump laser. The continuous-wave probe laser measures time of the heat dissipation (the decay time) from the suspended island through the NWs that support the island. To extract the thermal conductivity of NWs from the measured thermal decay time, we simulate the same experiment using the finite element method. In the simulations, the thermal conductivity of NWs acts as a free parameter to fit the experimentally measured heat dissipation curve. Our previous works^{17,18} describe this experimental technique in more details.

This is the author's peer reviewed, accepted manuscript. However, the online version of record will be different from this version once it has been copyedited and typeset.

PLEASE CITE THIS ARTICLE AS DOI: 10.1063/1.5130659

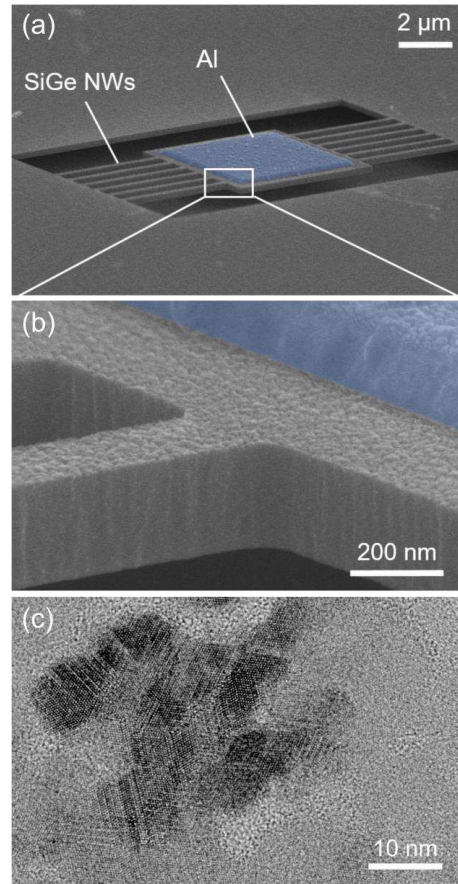


FIG. 1. SEM images of (a) typical μ TDTR sample with (b) a close-up view. (c) TEM image of $\text{Si}_{0.8}\text{Ge}_{0.2}$ sample showing polycrystallinity of the material.

Figure 1 shows a typical sample for the μ TDTR experiments. To fabricate our samples, we used conventional top-down fabrication techniques. First, a 300-nm-thick amorphous SiGe film was deposited on a thermally oxidized Si wafer by molecular beam epitaxy at room temperature. Then, we annealed the SiGe film at 850°C for 30 seconds in the N_2 atmosphere. As a result, we obtained the 300-nm-thick polycrystalline SiGe film with the grains of about 10 – 30 nm. Figure 1(c) shows a

This is the author's peer reviewed, accepted manuscript. However, the online version of record will be different from this version once it has been copyedited and typeset.

PLEASE CITE THIS ARTICLE AS DOI: 10.1063/1.5130659

transmission electron microscope image of the $\text{Si}_{0.8}\text{Ge}_{0.2}$ sample featuring multiple polycrystalline grains. Details about the crystallinity of Si and $\text{Si}_{0.5}\text{Ge}_{0.5}$ samples can be found in our previous works^{19,20}. Then, we deposited Al pads using the electron-beam lithography and the physical vapor deposition. Next, we created the NWs supporting the island by etching the SiGe layer using the electron-beam lithography and reactive ion etching. Finally, we removed the sacrificial SiO_2 layer under the structure by exposing the wafer to the vapor of hydrofluoric acid. To increase the precision of our experiments, we fabricated and measured each structure in three copies. Thus, the data points in this work show the average of three measurements with error bars indicating the standard deviation. More details on the fabrication methods can be found in our previous works^{9,21}.

This is the author's peer reviewed, accepted manuscript. However, the online version of record will be different from this version once it has been copyedited and typeset.

PLEASE CITE THIS ARTICLE AS DOI: 10.1063/1.5130659

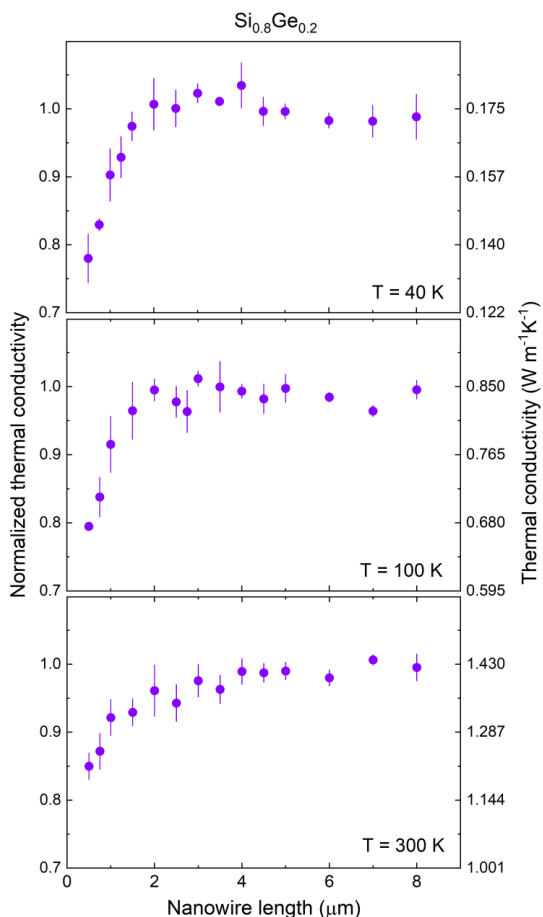


FIG. 2. Thermal conductivity of $\text{Si}_{0.8}\text{Ge}_{0.2}$ NWs at (a) 40 K, (b) 100 K, and (c) 300 K as a function of NW length.

First, we fixed the Ge composition at 20%, which is close to the concentration used in other works^{6,10}, and study the length dependence of thermal conductivity at different temperatures. Figure 2 shows the measured thermal conductivity of $\text{Si}_{0.8}\text{Ge}_{0.2}$ NWs as a function of the NW length. While the NWs longer than 2 μm show the constant thermal conductivity, the thermal conductivity of shorter NWs depends on their length. This dependence is the steepest at 4 K but flattens as the temperature is

This is the author's peer reviewed, accepted manuscript. However, the online version of record will be different from this version once it has been copyedited and typeset.

PLEASE CITE THIS ARTICLE AS DOI: 10.1063/1.5130659

increased. This behavior is similar to that of Si NWs⁹. Yet, even at room temperature, Si_{0.8}Ge_{0.2} NWs display the length-dependent thermal conductivity. The trend is similar to the theoretical predictions⁶ whereas the absolute values are 20% lower, possibly due to the polycrystallinity or higher surface roughness of our samples.

The ballistic heat conduction in SiGe is often attributed to the presence of Ge atoms in Si, which scatter high-frequency phonons by alloy scattering and thus leave heat conduction to the low-frequency part of phonon spectrum. Thus, the concentration of Ge in the Si matrix should have an impact on the strength of ballistic heat conduction and on the length dependence of thermal conductivity. Figure 3 shows the length-dependent thermal conductivity for the Ge concentration of 0%, 20%, and 50%. In the polycrystalline Si NWs without Ge (*i.e.* Si₁Ge₀), the thermal conductivity seems independent of the NW length. Indeed, even monocrystalline Si NWs display either very weak⁹ or no^{16,22} length dependence at room temperature. The polycrystalline grains in our samples can only further weaken this dependence, thus the absence of the length dependence is not surprising.

However, the NWs with 20% Ge concentration show a noticeable length dependence of their thermal conductivity despite the polycrystallinity (Fig. 3b). Further increase of Ge concentration to 50% strengthens the effect (Fig. 3c). These data seem to confirm the hypothesis that alloying strengthens the ballistic conduction due to scattering of the high-frequency phonons on heavier Ge atoms.

This is the author's peer reviewed, accepted manuscript. However, the online version of record will be different from this version once it has been copyedited and typeset.

PLEASE CITE THIS ARTICLE AS DOI: 10.1063/1.5130659

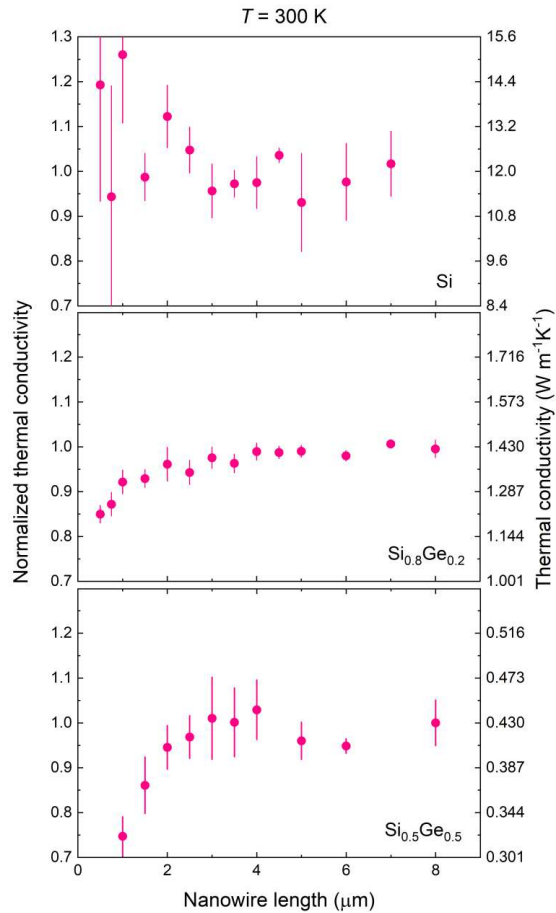


FIG. 3. Thermal conductivity of NWs with Ge composition of (a) 0%, (b) 20%, and (c) 50% as a function of the NW length.

The length dependence observed on $\text{Si}_{0.5}\text{Ge}_{0.5}$ NWs is proportional to $L^{0.4}$ for the shortest NWs. These results contrast with the data of Hsiao *et al.*¹⁰, who measured $\kappa \sim L^1$ dependence on both $\text{Si}_{0.9}\text{Ge}_{0.1}$ and $\text{Si}_{0.4}\text{Ge}_{0.6}$ NWs. Moreover, in the absolute values, we observe a typical U-shaped dependence^{23–25} of the thermal conductivity on Ge composition, whereas Hsiao *et al.*⁴ measured the same values of thermal conductivity at different Ge concentration.

To analyze the results more quantitatively, we fitted the length dependencies with polynomial functions $\kappa(L)$ and plotted its derivative $\alpha(L) = d \ln \kappa(L) / d \ln L$. Figure 4 shows the obtained $\alpha(L)$ dependencies for different compositions and temperatures. The temperature seems to have a minor impact of the strength of ballisticity, whereas the major impact comes from the Ge composition changing α from 0 to 0.4. The curve for $\text{Si}_{0.8}\text{Ge}_{0.2}$ closely resembles theoretical predictions by Upadhyaya and Aksamija⁶.

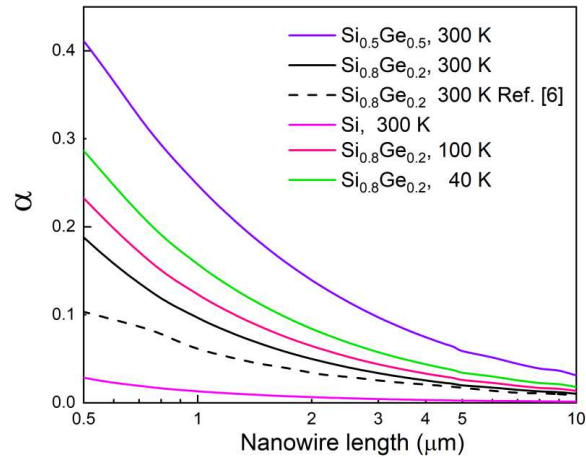


FIG. 4. Dependence of the α coefficient in $\kappa \sim L^\alpha$ dependencies measured experimentally in this work and obtained theoretically by Upadhyaya and Aksamija⁶.

Remarkably, both the theoretical prediction and the experimental result demonstrate a gradual decrease of α with the increase in length. This behavior differs from a sharp transition from $\alpha = 1$ to 0 at a certain length, which is sometimes expected²⁶ and observed in some experimental works^{10,27}. We explain the gradual reduction of α measured here and in our previous works^{9,15,16} by a wide range of phonon mean free paths (MFPs). While some phonons have long MFPs and can traverse a significant part of the NW ballistically, other phonons have short MFP and can conduct heat diffusely.

This is the author's peer reviewed, accepted manuscript. However, the online version of record will be different from this version once it has been copyedited and typeset.

PLEASE CITE THIS ARTICLE AS DOI: 10.1063/1.5130659

Thus, heat conduction remains semi-ballistic even over short distances about a few hundred nanometers. On the other hand, since $\alpha(L)$ dependencies approach $\alpha = 0$ asymptotically, heat conduction never becomes fully diffusive even in long NWs. For this reason, there cannot exist a certain length at which $\kappa(L)$ dependence becomes completely flat. Although experimentally we observe that the thermal conductivity becomes length-independent in long NWs, this only indicates that the sensitivity of our experiment becomes insufficient to probe fine $\kappa(L)$ dependence.

Moreover, phonon transport in nanowires resembles Levy walk^{6,9} in the direction parallel to the NW axis, thus the heat conduction would remain semi-ballistic even if all phonons had the MFP equal to the NW length.

In conclusion, we demonstrated semi-ballistic heat conduction in SiGe NWs shorter than 2 μm via the length-dependent thermal conductivity. We found that the concentration of Ge atoms plays an important role in this effect. The higher Ge concentration leads to a stronger length dependence of thermal conductivity. Moreover, the ballistic conduction becomes stronger as the temperature is decreased due to the increase of the wavelengths and MFPs of phonons. Analyzing the slope of the length dependence of thermal conductivity, we found a gradual transition from a diffusive to the semi-ballistic limit, in agreement with the theoretical predictions⁶. These findings help better understanding of heat conduction regimes in alloyed semiconductor nanostructures at different temperatures and alloy concentrations.

Acknowledgments

This work was supported by CREST JST (No. JPMJCR19Q3) and Kakenhi (Nos. 15H05869 and 17H02729)

References

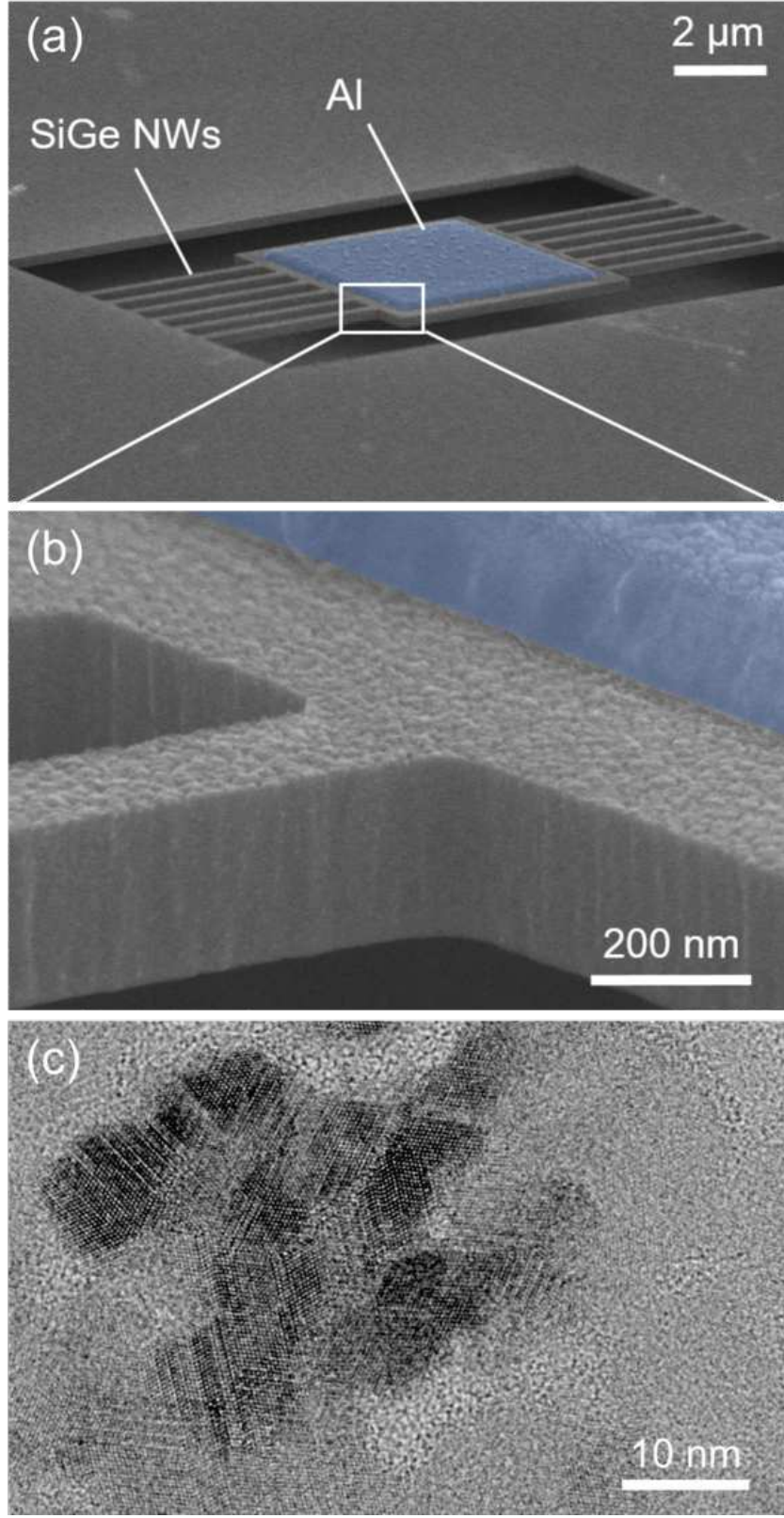
This is the author's peer reviewed, accepted manuscript. However, the online version of record will be different from this version once it has been copyedited and typeset.

PLEASE CITE THIS ARTICLE AS DOI: 10.1063/1.5130659

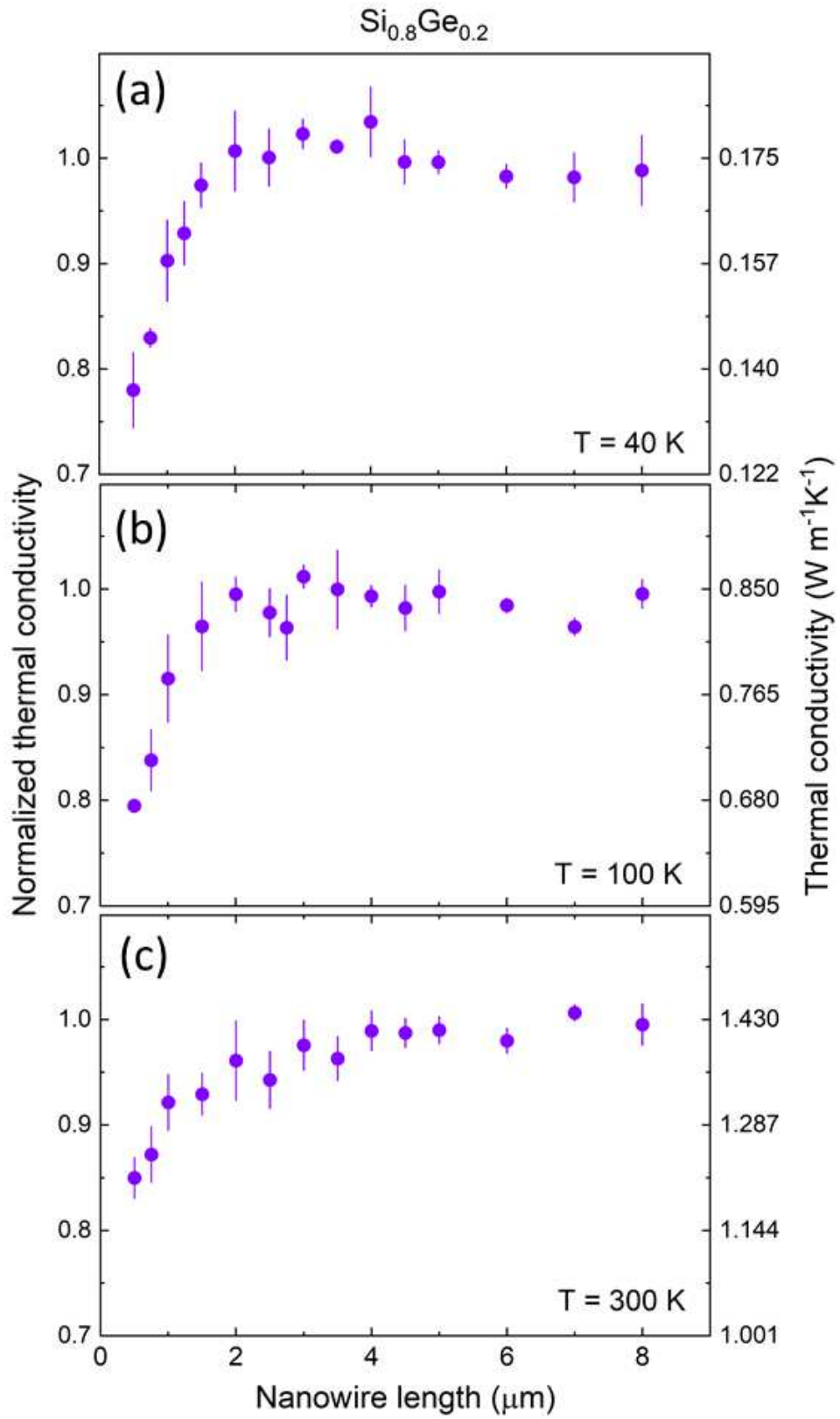
- ¹ M.E. Siemens, Q. Li, R. Yang, K.A. Nelson, E.H. Anderson, M.M. Murnane, and H.C. Kapteyn, *Nature Materials* **9**, 26 (2010).
- ² R.B. Wilson and D.G. Cahill, *Nature Communications* **5**, 5075 (2014).
- ³ N. Yang, G. Zhang, and B. Li, *Nano Today* **5**, 85 (2010).
- ⁴ L. Zeng, K.C. Collins, Y. Hu, M.N. Luckyanova, A.A. Maznev, S. Huberman, V. Chiloyan, J. Zhou, X. Huang, K.A. Nelson, and G. Chen, *Scientific Reports* **5**, 17131 (2015).
- ⁵ K.T. Regner, D.P. Sellan, Z. Su, C.H. Amon, A.J.H. McGaughey, and J.A. Malen, *Nature Communications* **4**, 1640 (2013).
- ⁶ M. Upadhyaya and Z. Aksamija, *Physical Review B* **94**, 174303 (2016).
- ⁷ J.A. Johnson, A.A. Maznev, J. Cuffe, J.K. Eliason, A.J. Minnich, T. Kehoe, C.M.S. Torres, G. Chen, and K.A. Nelson, *Physical Review Letters* **110**, 025901 (2013).
- ⁸ J.A. Johnson, J.K. Eliason, A.A. Maznev, T. Luo, and K.A. Nelson, *Journal of Applied Physics* **118**, 155104 (2015).
- ⁹ R. Anufriev, S. Gluchko, S. Volz, and M. Nomura, *ACS Nano* **12**, 11928 (2018).
- ¹⁰ T.-K. Hsiao, H.-K. Chang, S.-C. Liou, M.-W. Chu, S.-C. Lee, and C.-W. Chang, *Nature Nanotechnology* **8**, 534 (2013).
- ¹¹ T.K. Hsiao, B.W. Huang, H.K. Chang, S.C. Liou, M.W. Chu, S.C. Lee, and C.W. Chang, *Physical Review B* **91**, 035406 (2015).
- ¹² Q. Zhang, C. Liu, X. Liu, J. Liu, Z. Cui, Y. Zhang, L. Yang, Y. Zhao, T.T. Xu, Y. Chen, J. Wei, Z. Mao, and D. Li, *ACS Nano* **12**, 2634 (2018).
- ¹³ A. Tavakoli, K. Lulla, T. Crozes, N. Mingo, E. Collin, and O. Bourgeois, *Nature Communications* **9**, 4287 (2018).
- ¹⁴ A.A. Balandin, *Nature Materials* **10**, 569 (2011).
- ¹⁵ R. Anufriev, S. Gluchko, S. Volz, and M. Nomura, *Nanoscale* **11**, 13407 (2019).
- ¹⁶ J. Maire, R. Anufriev, and M. Nomura, *Scientific Reports* **7**, 41794 (2017).
- ¹⁷ J. Maire, R. Anufriev, T. Hori, J. Shiomi, S. Volz, and M. Nomura, *Scientific Reports* **8**, 4452 (2018).
- ¹⁸ R. Anufriev, R. Yanagisawa, and M. Nomura, *Nanoscale* **9**, 15083 (2017).
- ¹⁹ M. Nomura, Y. Kage, J. Nakagawa, T. Hori, J. Maire, J. Shiomi, R. Anufriev, D. Moser, and O. Paul, *Physical Review B* **91**, 205422 (2015).
- ²⁰ M. Nomura, J. Nakagawa, K. Sawano, J. Maire, and S. Volz, *Appl. Phys. Lett.* **109**, 173104 (2016).
- ²¹ R. Anufriev, A. Ramiere, J. Maire, and M. Nomura, *Nature Communications* **8**, 15505 (2017).
- ²² S.N. Raja, R. Rhyner, K. Vuttivorakulchai, M. Luisier, and D. Poulidakos, *Nano Letters* **17**, 276 (2016).
- ²³ S.N. Khatami and Z. Aksamija, *Physical Review Applied* **6**, 014015 (2016).
- ²⁴ M. Upadhyaya, S.N. Khatami, and Z. Aksamija, *Journal of Materials Research* **30**, 2649 (2015).
- ²⁵ S. Xiong, K. Säskilähti, Y.A. Kosevich, H. Han, D. Donadio, and S. Volz, *Physical Review Letters* **117**, 025503 (2016).
- ²⁶ C.-W. Chang, *AAPS Bulletin* **28**, 15 (2018).
- ²⁷ F. Zhuge, T. Takahashi, M. Kanai, K. Nagashima, N. Fukata, K. Uchida, and T. Yanagida, *Journal of Applied Physics* **124**, 065105 (2018).

This is the author's peer reviewed, accepted manuscript. However, the online version of record will be different from this version once it has been copyedited and typeset.

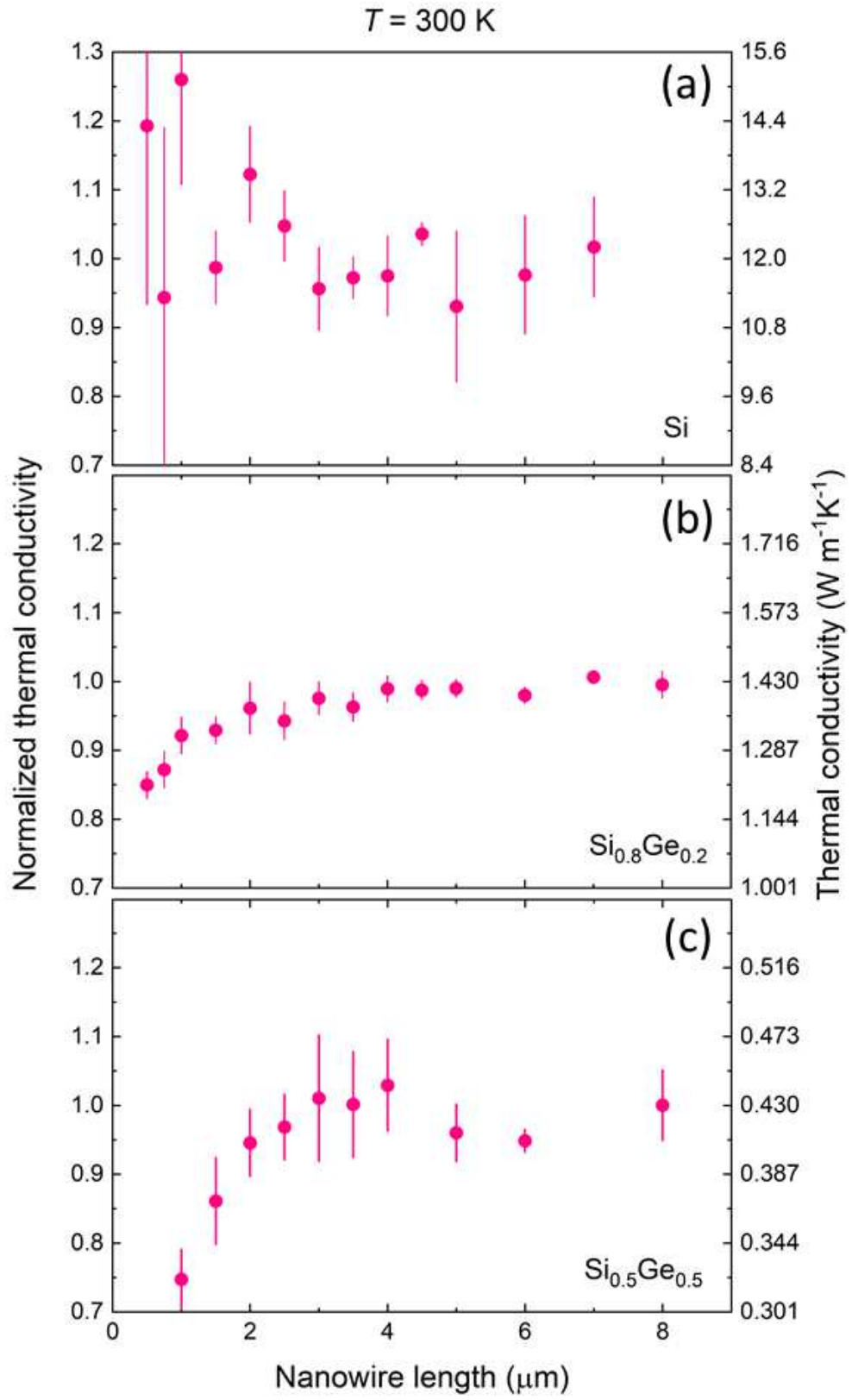
PLEASE CITE THIS ARTICLE AS DOI: 10.1063/1.5130659



This is the author's peer reviewed, accepted manuscript. However, the online version of record will be different from this version once it has been copyedited and typeset.
PLEASE CITE THIS ARTICLE AS DOI: 10.1063/1.5130659



This is the author's peer reviewed, accepted manuscript. However, the online version of record will be different from this version once it has been copyedited and typeset.
PLEASE CITE THIS ARTICLE AS DOI: 10.1063/1.5130659



This is the author's peer reviewed, accepted manuscript. However, the online version of record will be different from this version once it has been copyedited and typeset.

PLEASE CITE THIS ARTICLE AS DOI: 10.1063/1.5130659

